

## Formation of the amorphous phase in $Zr_2Al$ by hydrogen absorption and the effects of titanium substitution on the amorphization behaviour

Seung-Tae Ahn, Yong-Gyoo Kim and Jai-Young Lee

*Department of Materials Science and Engineering, Korea Advanced Institute of Science and Technology, Kusong-Dong 373-1, Yusung-Ku, Taejeon (South Korea)*

(Received December 2, 1991)

### Abstract

To explore the hydrogen-induced amorphization behaviour of  $Zr_2Al$  ( $Ni_2In$  type), the structural changes of the compound during hydrogen absorption are investigated by means of X-ray diffraction (XRD), transmission electron microscopy (TEM) and differential thermal analysis (DTA). To examine the effects of alloying element substitution, small amounts of zirconium are replaced by titanium, which has similar chemical and physical properties. At low reaction temperatures, the  $Zr_2Al$  and  $(Zr_{0.85}Ti_{0.15})_2Al$  compounds form crystalline hydride phases with orthorhombic structure initially, and then transform to an amorphous phase gradually. However, at higher temperatures they are decomposed into the stable phases  $ZrH_2$  and  $Zr_3Al_2$ . For the titanium-containing alloy, the reaction process and the amorphization mechanism are similar to those of the titanium-free alloy system. The amorphization temperature is increased by the titanium substitution, which is considered as being due to the increase of the elastic modulus owing to the titanium addition. It is suggested that the hydrogen-induced amorphization occurs as a result of the suppression of the decomposition of the crystalline hydride phase into the stable configurations, and the amorphization mechanism is the short-range motion of aluminium atoms.

### 1. Introduction

Some of intermetallic compounds are already known to become amorphized by hydrogen absorption [1]. Representative systems are  $RM_2$  (where R denotes rare earths and M denotes transition elements) Laves phases and zirconium-base compounds [2–5]. Of these the  $Zr_3Al$  compound with  $L1_2$  structure has a special interest because it can be amorphized by ion irradiation also [6–9]. Many researchers have proposed the elastic instability as a cause for amorphization of the compound during hydrogen absorption [7, 8].

It was reported that the  $Zr_2Al$  phase forms during the preparation of the  $Zr_3Al$  phase [6–8]. Thus the fact that  $Zr_3Al$  containing  $Zr_2Al$  as a second phase is thoroughly amorphized indicates the possibility of amorphizing the  $Zr_2Al$  system also. However, the amorphization behaviour of  $Zr_2Al$  due to hydrogen absorption has not been studied in detail.

Up to now, there is no report of the effects on the amorphization process of substitutions of different elements into hydrogen-absorbing metal systems.

Titanium forms a homogeneous solid solution with zirconium over the whole concentration range. As titanium has similar physical and chemical properties to zirconium, it is likely that the substitution of small amounts of titanium for zirconium leads to a homogeneous phase without disturbing the crystal structure. However, there are differences in the atomic radius and the elastic modulus. Titanium has a smaller atomic radius and a higher bulk modulus than zirconium. Thus substitution of titanium for zirconium is expected to affect the amorphization behaviour.

In this study, the hydrogen-induced amorphization behaviour of  $Zr_2Al$  is investigated. Subsequently the crystallization process of the amorphous phase is studied by differential thermal analysis (DTA). The amorphization of the  $(Zr_{0.85}Ti_{0.15})_2Al$  phase is studied in order to determine the effects of titanium addition. Finally an amorphization mechanism is proposed on the basis of the results obtained.

## 2. Experimental details

The intermetallic compounds  $Zr_2Al$  and  $(Zr_{0.85}Ti_{0.15})_2Al$  were prepared by arc melting in argon atmosphere using pure zirconium (99.7%), titanium (99.9%) and aluminium (99.99%). To ensure homogeneity, the samples were remelted several times, and then heat treated in vacuum ( $10^{-4}$  Torr) at 1213 K for 10 days. The sample identification was done through X-ray diffraction (XRD) tests using  $Cu\ K\alpha$  radiation.

Before hydrogenation, the sample was crushed to powder below 100 mesh. Hydrogen absorption was carried out in a Sievert-type apparatus, varying the charging conditions. The hydrogen pressure was fixed to 50 atm  $H_2$  in all experiments.

The structural changes induced by the hydrogen absorption were basically checked by XRD. To confirm the amorphous structure, some of the samples were further examined by transmission electron microscopy (TEM) using a JEOL 200CX instrument. The TEM sample was prepared by crushing it in acetone.

The crystallization behaviour of the amorphous samples was examined by DTA in an argon atmosphere with a heating rate of  $20\ K\ min^{-1}$ . The DTA curves were corrected by subtracting the base line, which was obtained on a standard sample of pure alumina powder. The nature of the crystallization products was determined by XRD on specimens heated to the crystallization temperatures, or to temperatures higher than the reaction peaks in the DTA curves.

## 3. Results

Figure 1 shows the XRD patterns of  $Zr_2Al$  compound before and after the hydrogenation treatments at various temperatures for 48 h. The as-

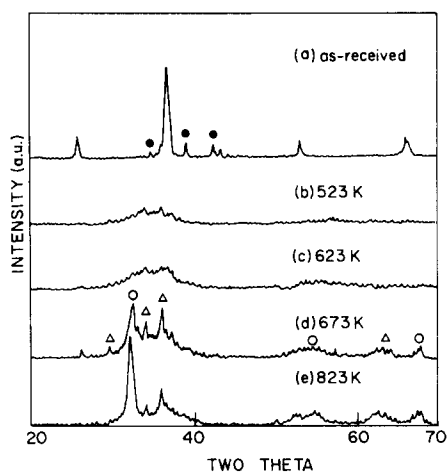


Fig. 1. XRD patterns of  $Zr_2Al$  before and after hydrogenation treatments at various temperatures for 48 h: ●,  $Zr_3Al$ ; ○,  $ZrH_2$ ; △,  $Zr_3Al_2$ .

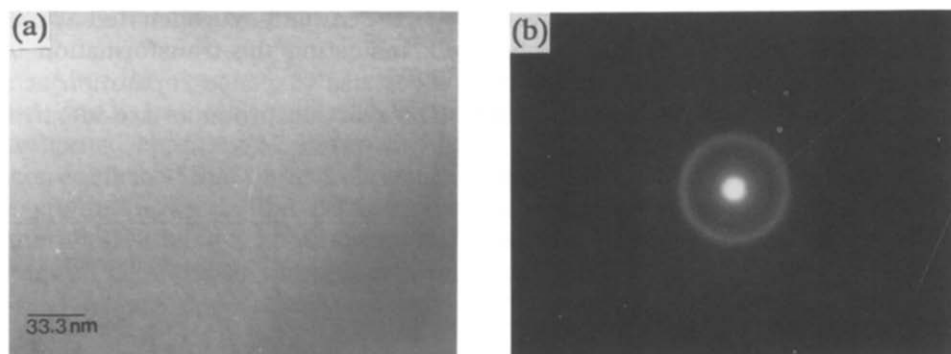


Fig. 2. (a) Bright-field image and (b) the corresponding electron diffraction pattern for the sample hydrogenated at 523 K for 48 h.

received sample contains small amounts of  $Zr_3Al$  phase as a second phase. The major portion is the well-defined  $Zr_2Al$  phase of hexagonal structure having the lattice parameters  $a = 4.88 \text{ \AA}$  and  $c = 5.97 \text{ \AA}$ . After the hydrogenation the crystalline Bragg peaks are no longer observed in the temperature ranges around 523 and 623 K. The patterns with broad maxima indicate that transformation to an amorphous state may have taken place. However, at higher temperatures some new reflections on top of the broad maxima are observed, and they are indexed as belonging to  $ZrH_2$  and  $Zr_3Al_2$ . For the sample hydrogenated at 523 K, a transmission electron micrograph and the corresponding diffraction pattern are shown in Fig. 2. The featureless image and the diffuse halo ring clearly show that the sample is at least amorphous.

From Fig. 1, it is uncertain whether the sample forms a crystalline hydride phase before amorphization. In the case of  $Zr_3Al$ , there was no

apparent crystalline hydride phase during hydrogen absorption [7, 8]. Hydrogen absorption in  $Zr_2Al$  has hardly taken place at temperatures below 523 K. For simplicity, hydrogen absorption was carried out at 523 K for a short time. In Fig. 3, XRD patterns for different charging times are shown after hydrogenation at 523 K. After 10 h, there are two distinct crystalline phases. One of these is the unhydrogenated  $Zr_2Al$  phase and the other is the crystalline hydride phase. Recently Clark and Wu reported that  $Zr_2Al$  can absorb hydrogen up to  $[H]/[M]=2.8$ , *i.e.*  $Zr_2AlH_{2.8}$ , at ambient conditions [10]. This phase was identified as having an orthorhombic structure with the lattice parameters  $a=8.689 \text{ \AA}$ ,  $b=5.358 \text{ \AA}$ ,  $c=6.006 \text{ \AA}$ . Our result is well in accord with their work. Thus the amorphization of  $Zr_2Al$  during hydrogen absorption is through the crystalline hydride state and the mechanism is different from that of the  $Zr_3Al$  system.

XRD patterns of a titanium-substituted sample, taken after applying different charging temperatures, are shown in Fig. 4. The as-received sample also adopts the hexagonal structure, but with smaller lattice constants than  $Zr_2Al$  due to the smaller atomic radius of titanium than zirconium ( $a=4.83 \text{ \AA}$ ,  $c=5.88 \text{ \AA}$ ). By hydrogenation, the original crystalline phase gradually disappears and broad maxima develop. For the sample hydrogenated at 623 K, only the broad maximum is observed, indicating the transformation to an amorphous phase. Also this system gives rise to phase separation at a reaction temperature as high as 723 K. The reaction products are identical

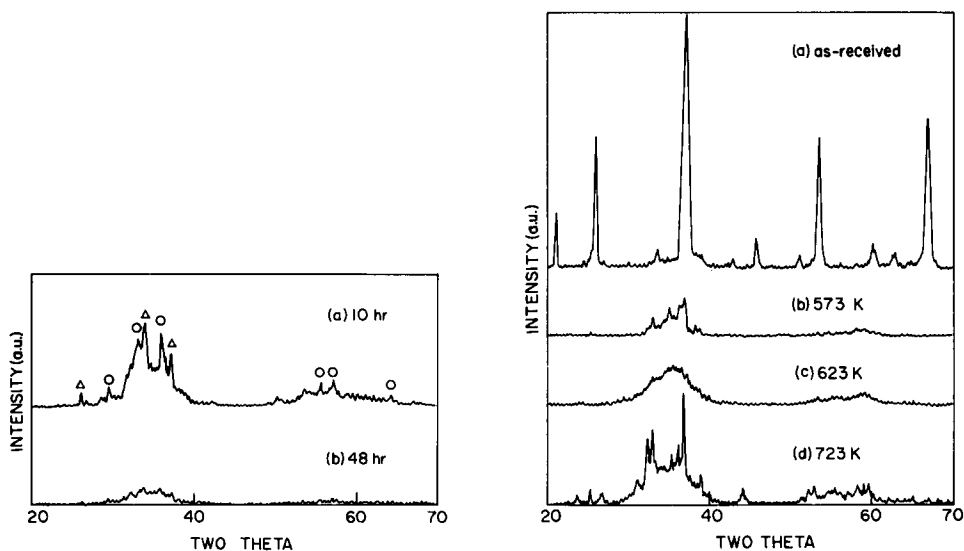


Fig. 3. XRD patterns of  $Zr_2Al$  for various reaction times when hydrogenated at 523 K.  $\circ$ , unhydrogenated phase;  $\Delta$ , crystalline  $Zr_2AlH_{2.8}$  phase.

Fig. 4. XRD patterns of  $(Zr_{0.85}Ti_{0.15})_2Al$  before and after hydrogenation treatments at various temperatures for 48 h.

to those of  $Zr_2Al$  phase. The overall transformation behaviour of this alloy system during hydrogen absorption is similar, regardless of titanium addition.

It should be noted that only partial amorphization occurs at 573 K, while the titanium-free sample has already converted to the amorphous state at 523 K. This indicates that the amorphization reaction becomes slower when Ti atoms are substituted. The nature of the retardation of reaction will be discussed in the next section.

The thermal behaviour of amorphous phases was investigated and is shown in Fig. 5. The broken line in the figure is the corrected baseline. The titanium-free sample shows one exothermic reaction at around 900 K followed by a small endothermic reaction. In the case of titanium-containing amorphous phases, the exothermic reaction starts at lower temperatures and the exotherms are broadened. Two exothermic reactions are observed. The first peak has the same peak temperature as the titanium-free specimen. Also an endothermic reaction is observed after the exothermic reaction. These endothermic reactions revealed in the DTA traces may be caused by the desorption of hydrogen. To examine the structural change of the sample during each of these exothermic reactions, the samples were quenched from the temperatures indicated by arrows, and then XRD tests were performed. The results are shown in Fig. 6.

After the reaction, some crystalline phases are found and they are  $ZrH_2$  and  $Zr_3Al_2$  in both cases. These products are identical to the cases of isothermal charging as shown in Figs. 1 and 4. Before the reaction, it had been confirmed that the sample was still amorphous. Therefore the exothermic reactions shown in the DTA curves are due to the crystallization of the amorphous phase. The amorphous phase that contained small amounts of titanium crystallized through two reaction steps.

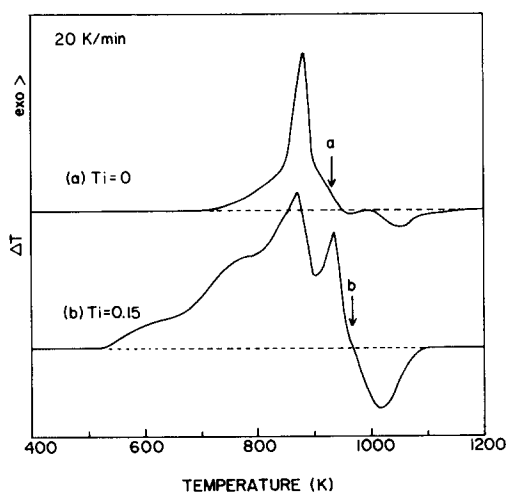


Fig. 5. DTA curves for the titanium-free (upper curve) and titanium-containing (lower curve) amorphous phases ( $20\text{ K min}^{-1}$ ): ---, corrected base lines.

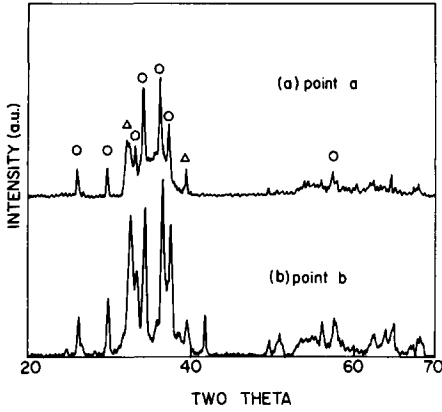


Fig. 6. XRD patterns of the samples quenched from the temperatures indicated by arrows in the DTA. O,  $ZrH_2$ ;  $\Delta$ ,  $Zr_3Al_2$ .

#### 4. Discussion

The increase of the amorphization temperature due to titanium substitution has been examined as follows. Recently, Kim found that the amorphization temperature of the Laves phase  $ErCo_2$  was decreased by substitution of manganese or iron for cobalt [11]. He interpreted these results as being due to a decrease of the activation energy for the transformation. The activation energy was suggested to be closely related to the elastic modulus and the heat of formation of the compound. As the elastic modulus (especially bulk modulus) or heat of formation  $\Delta H_f$  were larger in absolute value, the amorphization temperature was higher. Also Chung *et al.* pointed out the importance of the elastic modulus on the amorphization mechanism of Laves phases composed of rare earths and transition elements such as nickel and iron [5]. Titanium has a higher bulk modulus than zirconium (108.4 GPa, and 89.8 GPa respectively). Thus the addition of titanium into  $Zr_2Al$  would lead to an increase of the elastic modulus of the compound and to stronger resistance against amorphization.

Secondly the heat of formation of the compound is considered. In this work,  $\Delta H_f$  is calculated using the Miedema model [12]. The  $\Delta H_f$  of a ternary system is obtained from the following method of dividing into binary systems:

$$\Delta H_f(Zr_2Al) = -63.9 \text{ kJ mol}^{-1}$$

$$\begin{aligned} \Delta H_f((Zr_{0.85}Ti_{0.15})_2Al) &= 0.85\Delta H_f(Zr_{0.57}Al_{0.28}) + 0.15\Delta H_f(Ti_{0.1}Al_{0.05}) \\ &\quad + \Delta H_f(Zr_{0.57}Ti_{0.1}) \\ &= -61.9 \text{ kJ mol}^{-1} \end{aligned}$$

$\Delta H_f$  of the compound increases very slightly with the addition of titanium. This increase may make the amorphization temperature lower. However, the actual amorphization temperature is increased by the titanium addition. Thus

it is thought that the change of the elastic modulus due to the substitution brings about a major contribution to the amorphization of the  $Zr_2Al$  system.

Let us consider the amorphization mechanism of the  $(Zr, Ti)_2Al$  compounds. As shown in Fig. 3, the amorphous phase is formed from the crystalline hydride phase. To investigate the reaction mechanism, a kinetic study should be carried out. Some authors have done kinetic measurements on  $Zr_3Rh$  [13, 14] and  $ErNi_2$  [15]. Yeh and Johnson [14] proposed from the X-ray intensity measurements that the amorphization mechanism of  $Zr_3Rh$  is the interface-controlled reaction through the motion of metal atoms. Chung and Lee [15] suggested that amorphization of  $ErNi_2$  is controlled by the transition element (nickel), which has a smaller atomic radius than the Er atom. In other words, the dominant moving species are metal atoms, not hydrogen atoms at all.

Thus it can be said that the amorphization of  $Zr_2Al$  is controlled by the motion of metal atoms. The ratio of atomic radii between aluminium and zirconium ( $r = r_{Al}/r_{Zr}$ ) is 0.894 when expressed in Goldschmidt radii. Because of this smaller atomic size of aluminium, the movement of aluminium atoms as the dominant controlling process is thought to be a reasonable possibility. Were this motion to involve long-range diffusion, the system would become equilibrated so that stable phases are formed as shown in Figs. 1(d) and 1(e). However, long-range metal atom diffusion must be hampered because of the relatively low reaction temperature so that the system remains in the intermediate state, *i.e.* the amorphous state. When considering the presence of the crystalline hydride phase, it is believed that formation of the amorphous phase is the thermally activated process as indicated by Chung and Lee [15]. The mechanism and the reaction process are clearly different from those found in the  $Zr_3Al$  compound [8]. However, the reasons why these two systems differ cannot be given at present.

## 5. Summary

The observations made with regard to the hydrogen-induced amorphization of  $Zr_2Al$  can be summarized as follows.

(1)  $Zr_2Al$  can be amorphized by hydrogen absorption after the formation of the crystalline  $Zr_2AlH_{2.8}$  phase. At high reaction temperatures, it decomposes into  $ZrH_2$  and  $Zr_3Al_2$  as final equilibrium products.

(2) For a sample containing titanium as a third element, amorphization is also observed and the final products are the same as for the titanium-free sample. The titanium-containing sample shows the amorphization phenomenon at a somewhat higher reaction temperature than for  $Zr_2Al$ . It is suggested that the increase of the amorphization temperature is caused by the increase of the elastic modulus by a titanium addition.

(3) The titanium-free amorphous phase crystallizes through a one-step reaction, but the titanium-containing sample crystallizes through a two-step process. The amorphous phases, whether titanium is absent or not, decompose

into  $ZrH_2$  and  $Zr_3Al_2$ . These products are identical to those of isothermal hydrogenation treatments.

(4) It is suggested that the amorphization is controlled by the motion of aluminium atoms, which have smaller atomic radii than the zirconium atom.

### Acknowledgment

The financial support of the Korea Science and Engineering Foundation (KOSEF) is gratefully acknowledged.

### References

- 1 X. L. Yeh, K. Samwer and W. L. Johnson, *Appl. Phys. Lett.*, **42** (1983) 242.
- 2 R. C. Bowman, Jr., J. S. Cantrell, K. Samwer, J. Tebbe, E. L. Venturini and J. J. Rush, *Phys. Rev. B*, **37** (1988) 8575.
- 3 K. Aoki, T. Yamamoto and T. Masumoto, *Scripta Metall.*, **21** (1987) 27.
- 4 K. Aoki, A. Yanagitani, X. G. Li and T. Masumoto, *Mater. Sci. Eng.*, **97** (1988) 35.
- 5 U. I. Chung, Y. G. Kim and J. Y. Lee, *Philos. Mag. B*, **63** (1991) 1119.
- 6 P. R. Okamoto, L. E. Rehn, J. Pearson, R. Bhadra and M. Grimsditch, *J. Less-Common Met.*, **140** (1988) 231.
- 7 W. J. Meng, P. R. Okamoto, L. J. Thompson, B. J. Kestel and L. E. Rehn, *Appl. Phys. Lett.*, **53** (1988) 1820.
- 8 J. Y. Lee, W. C. Choi, Y. G. Kim and J. Y. Lee, *Acta Metall. Mater.*, **39** (1991) 1693.
- 9 L. M. Howe and M. H. Rainville, *J. Nucl. Mater.*, **68** (1977) 215.
- 10 N. J. Clark and E. Wu, *J. Less-Common Met.*, **166** (1990) 7.
- 11 Y. G. Kim, *Ph.D. Thesis*, Korea Advanced Institute of Science and Technology, Yuseong-Ku, Taejon, 1992.
- 12 A. K. Niessen, F. R. de Boer, R. Boom, D. F. de Chatel, W. C. M. Mattens and A. R. Miedema, *CALPHAD*, **7** (1983) 51.
- 13 K. Samwer, in G. Bambakids and R. C. Bowman, Jr., (eds.), *Hydrogen in Disordered and Amorphous Solids*, Plenum, New York, NY, 1986, p. 173.
- 14 X. L. Yeh and W. L. Johnson, *Caltech Rep. 10870-157*, 1985.
- 15 U. I. Chung and J. Y. Lee, *Acta Metall. Mater.*, **38** (1990) 811.